STATISTICAL EVALUATION OF MECHANICAL PROPERTIES OF TETRACALCIUM PHOSPHATE BASED CEMENTS

Ľ. Medvecký, M. Kašiarová, J. Mihalik, T. Sopčák, H. Bruncková, J. Briančin

Abstract

CPC cements were prepared by mixing a tetracalcium phosphate and dicalcium phosphate powder mixture with 1.5 M KH_2PO_4 hardening liquid. Samples were hardened in simulated body fluid at 37°C for 1 week. Both the compressive and diametral tensile strengths were evaluated in relationship to the reproducibility of tetracalcium phosphate properties. Significant statistical differences in mechanical properties were found despite the same preparation procedure being used for tetracalcium phosphate. Dissimilar TTCP particle size distribution curves after milling with various volume fractions of larger TTCP agglomerates were probably the reason for these differences.

Keywords: calcium phosphate cement, tetracalcium phosphate, compressive strength, diametral tensile strength, particle size distributions

INTRODUCTION

Calcium phosphate cements (CPCs) represent a class of biomaterials which have been discovered by LeGeros et al. [1], Brown and Chow [2]. Because of the excellent biocompatibility and osteoconductivity, CPCs have been used as filling materials in many dental and medical applications [3-5]. In general, CPCs are composed of one or more calcium orthophosphates, which form a moldable paste by mutual mixing with the hardening liquid. One group of the CPC is based on tetracalcium phosphate, which is mixed with dicalcium phosphate (anhydrous (DCPA) or dihydrate (DCPD)) and calcium-deficient hydroxyapatite (CDHA) is the end product of hardening through dissolution-precipitation reactions [6]. The strength of cements is affected by various factors like the particle size of the starting cement precursors [7], the powder to liquid ratio (P/L) and the chemical nature of hardening liquids, or additives [8]. From the point of view of diametral tensile strength (DTS), the optimal CPC powder to hardening liquid was 4 (CPC DTS about 13 MPa) [7]. Hirayama et al. [9] studied the effect of TTCP/DCPA molar ratio on the cement DTS after immersing in a physiological-like solution and revealed that the DTS decreased from 11.7 MPa to 7.2 MPa with decreasing TTCP/DCPA molar ratios from 1/1 to 1/3. In the study of Dagang et al. [10] the cement reached a maximum compressive strength (CS) of 55 MPa at the optimal P/L ratio of 3.7. Burguera et al. [11] developed a CPC comprised from TTCP/DCPD powders with particle sizes (17 and 1.7 μm, respectively) with water or sodium phosphate as hardening liquids at P/L = 4. In our previous work (Medvecký et al. [12]), the CPC CS achieved up to 80 MPa at P/L = 2 and cement paste pressing at 6 MPa.

From the viewpoint of practical utilization of the TTCP based cements, and generally significant differences in measured mechanical properties in the works, we

Ľubomír Medvecký, Monika Kašiarová, Ján Mihalik, Tibor Sopčák, Helena Bruncková, Institute of Materials Research, Slovak Academy of Sciences, Košice, Slovak Republic
Jaroslav Briančin, Institute of Geotechnics, Slovak Academy of Sciences, Košice, Slovak Republic

evaluated the reproducibility of TTCP properties in relationship to mechanical properties and microstructure of the final cement in this paper. Three TTCP powders were prepared by the same procedure and their morphology, phase purity, and particle size distributions were compared.

EXPERIMENTAL

Materials

Three individual tetracalcium phosphate ($Ca_4(PO_4)_2O$, TTCP) powder phases were prepared by annealing an equimolar mixture of calcium carbonate ($CaCO_3$ (analytical grade), Sigma Aldrich) and dicalcium phosphate dihydrate (DCPD) ($CaHPO_4 \cdot 2H_2O$ (Ph.Eur.), Fluka) at 1420°C for 4 hours. After cooling, the product was kept in a desiccator at room temperature. The same TTCP amounts were crushed by milling in a planetary ball mill (Fritsch, ZrO_2 balls and vessel) for 2 hours. The particle size distributions of the TTCP and dicalcium phosphate anhydrous (DCPA, Sigma Aldrich, analytical grade) were measured in methanol by a laser scattering particle size analyzer (SYMPATEC HELOS). A bimodal distribution curve was measured in the case of DCPA precursor with two maxima around 2 and 20 μm (d_{50} = 2.5 μm). The cement powder mixtures were composed of TTCP and DCPA in an equimolar ratio. The 1.5 M KH_2PO_4 (analytical grade, Merck) solution was applied as a hardening liquid and the powder/liquid ratio equalled 2.

After hardening the liquid addition to the powder mixture, resulting pastes were packed in stainless cylindrical form (6 mm D × 12 mm H) and hardened in 100% humidity at 37°C for 10 min. The samples were consequently soaked in simulated body fluid (SBF, prepared according to [13], V_{SBF} = 100 ml) at 37°C for 1 week. The final discs were dried at 80°C for 2 hours after washing with distilled water.

The diametral tensile strength of samples was measured according to [14]. The discs had dimensions of 6 mm in diameter and 3 mm in length. For each experimental group, the compressive strength and diametral tensile strengths were measured for 10 samples on a universal testing machine (LR5K Plus, Lloyd Instruments Ltd.) at a crosshead speed of 1 mm/min and 10 mm/min respectively. The mean value and standard deviation of each measured property were calculated for each group of ten specimens. The analysis of variance (ANOVA) was used. Statistical significance was considered at $P > 0.05$. The phase composition of samples was analyzed by X-ray diffraction analysis (Philips X´ PertPro, using Cu Kα radiation), FTIR spectroscopy (Shimadzu, IRAffinity1, 400 mg KBr + 1 mg sample). The microstructures of fractured surfaces of samples were observed by field emission scanning electron microscopy (JEOL FE SEM JSM-7000F). Densities of samples were calculated from their weights and dimensions. The setting times (ST) of the cement pastes were evaluated using the tip (1 mm diameter) of a Vicat needle with a 400 g load (according to ISO standard 1566), and fails to make a perceptible circular indentation on the surface of the cement.

RESULTS AND DISCUSSION

The phase compositions of TTCP powders after milling are shown in Fig.1. From the figure it results that all prepared TTCP precursors are monophasic (JCPDS 25-1137) with the same crystallinity of particles. The analysis of TTCP particle size distributions verified small differences between individual powders (Fig.2). In samples 2 and 3 bimodal distribution curves were observed, whereas the monomodal distribution curve was measured in sample 1. The maxima of bimodal curves were located around 6 and 90 μm in sample 3; 6 and 80 μm in sample 2. In the case of sample 1, the maximum distribution

curve was found only at 6 μm. The large TTCP particle agglomerates with dimensions above 50 μm represented approximately 10 vol.% and 5 vol.% in sample 3 and 2 respectively. The average dimension of particles d_{50} were 5.34, 5.65 and 5.96 in samples 1, 2 and 3, from which it results that the presence of a small amount of coarser particle fractions insignificantly influences this parameter.

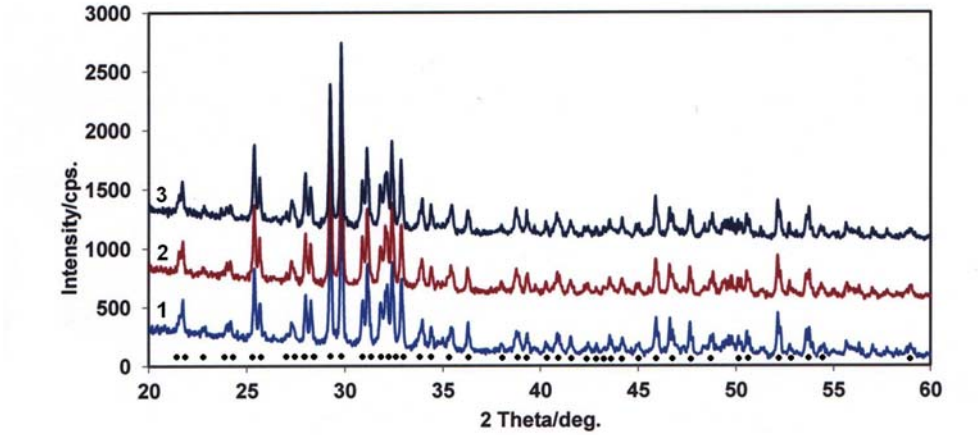

Fig.1. XRD patterns of TTCP powder samples after milling. (● TTCP phase (JCPDS 25-1137)).

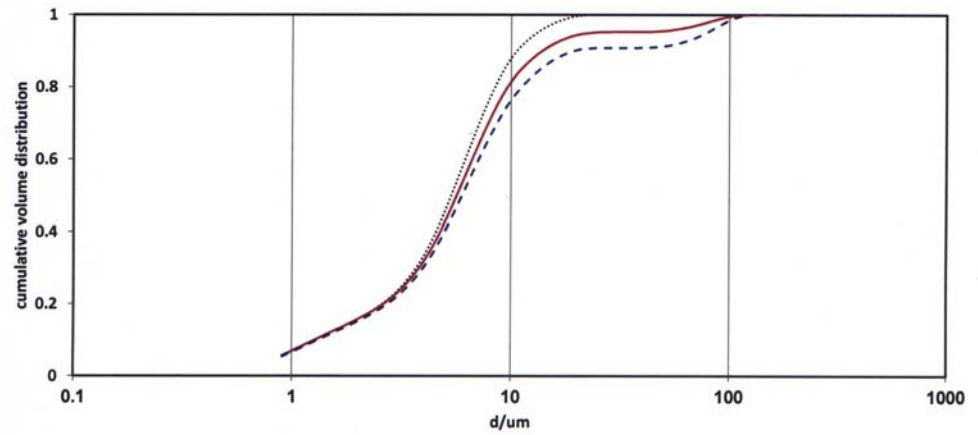

Fig.2. Cumulative particle size distribution of TTCP particles in prepared and milled phases. (…. sample 1, ___ sample 2, ---- sample 3).

The XRD diffraction patterns of cements after hardening at 37°C for 1 week are shown in Fig.3. From a comparison of patterns it is clear that the major phase represents the calcium deficient nanocrystalline hydroxyapatite phase (JCPDS 9-432). Besides this, small fractions (<7 vol.%) of starting TTCP and DCPA cement phases are visible in patterns of all cements. No brushite lines were visible in XRD patterns and no significant differences in the phase composition of hardened cements were found.

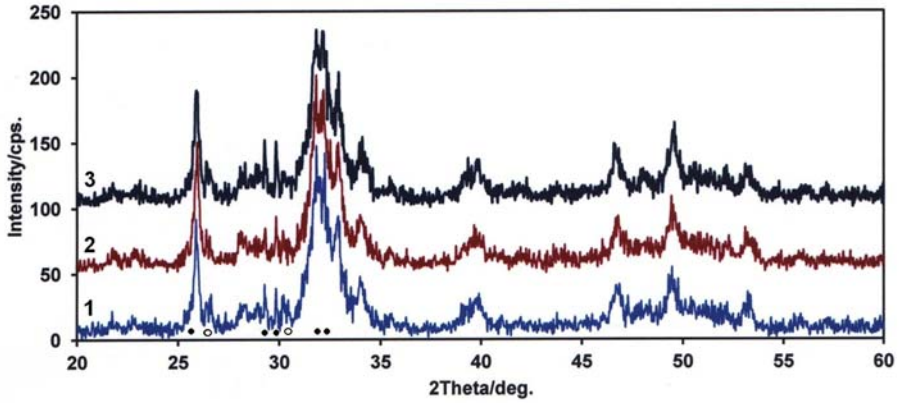

Fig.3. XRD patterns of cements after hardening at 37°C for 1 week in SBF. (● TTCP phase, ○ DCPA phase (JCPDS 09-0080), unmarked lines represent nanohydroxyapatite).

In the IR spectra of cements after 7 days of hardening in SBF (Fig.4), there were observed weak intensive bands at wavenumbers between 400-500 cm^{-1} that characterize ν_2 TTCP vibrations [15], ν_4, ν_3, ν_1 vibrations of PO_4 bands (1060 (ν3), 1100 (ν3), 960 (ν1), 570 (ν4), 600 (ν4) cm^{-1}), the peak at 3570 and the shoulder around 630 cm^{-1} from stretching and librational OH hydroxyapatite vibrations [16]. Apart from the ν_3 vibrations (at 1420 and 1470 cm^{-1}), ν_2 of CO_3^{2-} group (at 870 cm^{-1}) and vibrations of adsorbed H_2O molecules at 1630 cm^{-1} can be visible in spectra [17]. The vibrations of CO_3^{2-} group correspond with vibrations in the B-type of carbonated hydroxyapatite. No significant differences between IR spectra of samples were observed besides a small increase in the carbonate content in cement 1. Thus from the above, we believe that the main problem from the viewpoint of the reproducibility of TTCP properties is obtaining powders with the same particle size distribution after milling.

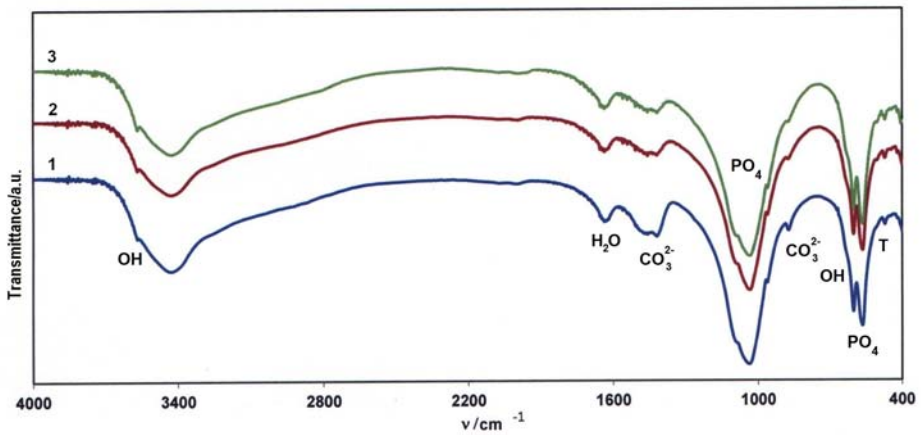

Fig.4. IR spectra of cements after hardening at 37°C for 1 week in SBF. (T-TTCP residua).

The TTCP particles had irregular morphology or were prolonged in shape with dimensions between 1-20 μm (Fig.5). In microstructures of cements 1 and 2, extremely fine apatite particles with needle-like morphology were found (Fig.6).

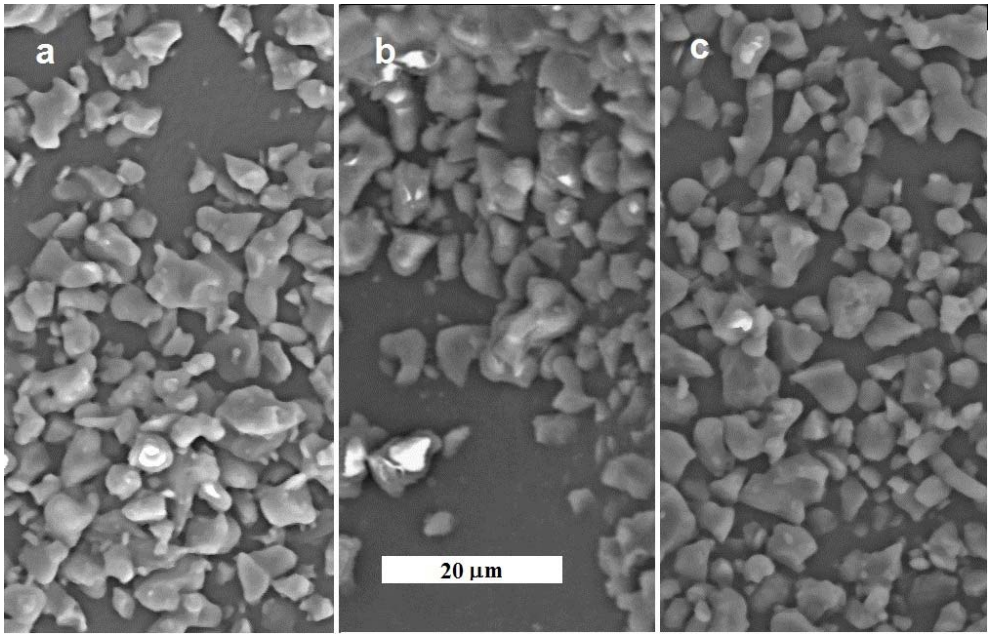

Fig.5. SEM image of TTCP particle morphology after milling.

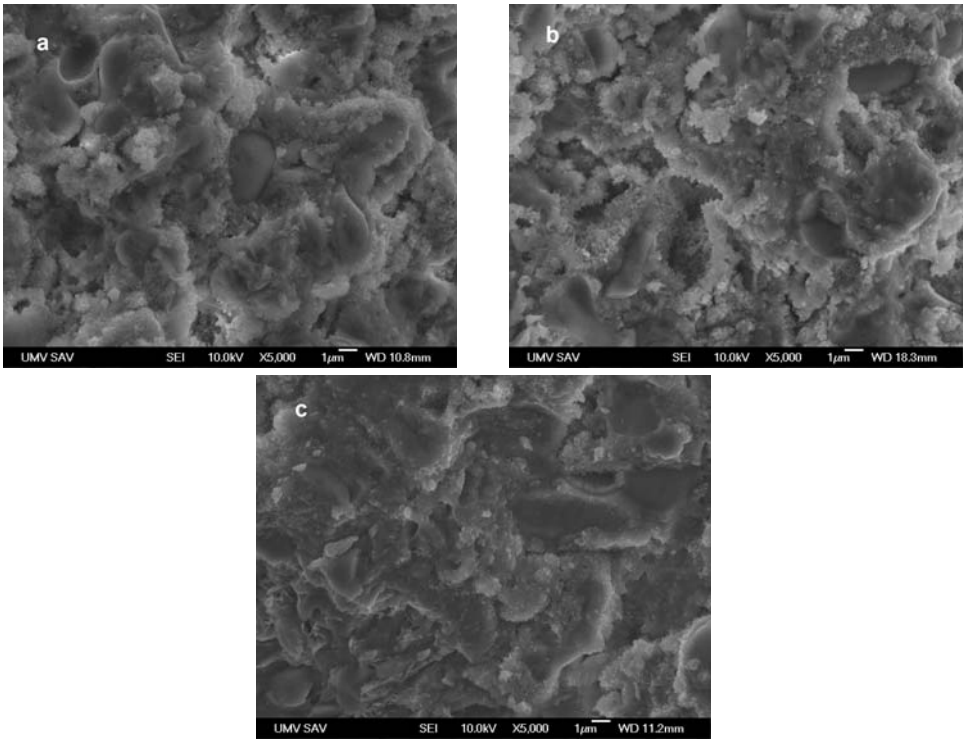

Fig.6. Microstructures of biocements after hardening at 37°C for 1 week in SBF.

The length of particles in cement 1 was up to 60 nm and diameter did not exceed 40 nm, on the other hand, the particle length was up to 100 nm in cement 2. Besides this, the larger denser irregularly shaped particles with dimensions around 2 μm are visible in both cement microstructures. From detailed analysis it results that these particles represent the residua of the starting TTCP particles in cement powder mixtures, which are surrounded by a new hydroxyapatite phase – the needle-like and spherical (inside large particles) morphology. Note that the TTCP phase is only present in the core of particles because there was found a small content of untransformed TTCP fraction in cements on basis of XRD analysis. In the case of cement 3, the needle-like hydroxyapatite particles were not observed in the microstructure. The microstructure is composed from denser larger agglomerates of fine globular hydroxyapatite particles and individual boundaries between agglomerates are not clearly distinguished, which confirms their more coherent character and a stronger mutual interconnection. The porosities and pore morphologies were very similar in cement microstructures 1 and 2. Pores had irregular shapes and practically two different types of pores were found – the fine pores with dimensions up to 1 μm and the large pores (up to 5 μm), which are formed after the full dissolution and transformation of DCPD or TTCP particles. Large pores are surrounded by needle-like nanohydroxyapatite particles after dissolution/precipitation processes. In cement 3, the small pores (around 2 μm) represent the major pore fraction and pores have more compact boundaries composed of a fine globular nanohydroxyapatite matrix. The setting times of cements were 5 minutes.

Tab.1. Statistical evaluation of cement properties.

sample	CS [MPa]	DTS [MPa]	Density [g·cm^{-3}]
1	44 ± 6.4	3.5 ± 0.80	1.73 ± 0.027
2	48 ± 14	4 ± 1.54	1.77 ± 0.029
3	59 ± 6.3	2.05 ± 0.81	1.76 ± 0.021

In Table 1 the results of the analysis of mechanical properties - compressive strength (CS) and diametral tensile strength (DTS) are shown. On the basis of statistical evaluation (ANOVA, one-way), there are significant differences between the CS´s of cement samples ($p<0.024$). The CS average values of cements were 44, 48 and 59 MPa, where the highest STD was measured in cement 2 (approx. 14 MPa). In the case of DTS values, similarly significant differences were found among cement DTS ($p<0.002$). The DTS values were 3.5, 4 and 2.05 MPa with the highest STD value in cement 2. Significant differences were verified between values of cement densities ($p<0.006$) as well. The highest density was measured in cement 2 (1.77 g·cm^{-3}) and the density of the cement 1 significantly differs from others. It is clear from Tab.1 that no correlations between CS (DTS) and density of samples are visible. CS and DTS values of TTCP based cements with H_3PO_4 as the hardening liquid and P/L ratio equalling 4 were 50 and 7.5 MPa respectively [18], contrary to the DTS value of 6.2 MPa [14] in cement with a mole ratio of TTCP/DCPA=3/1. Note that in this work the mean particle sizes of TTCP and DCPA powder precursors were 11 and 0.6 μm.

The mechanical properties of cements were affected mainly by the formed cement microstructure, because only small differences in TTCP phase characteristics were observed. The microstructure of the final cements was influenced by the presence of a fraction of coarser TTCP particles – a denser microstructure with a lower degree of needle-like hydroxyapatite particles formation was found. This type of microstructure is

appropriate for achievement of higher CS´s, but DTS values were much lower than in cements with microstructure in which needle – like particles were formed. Cement 3, with compactness of microstructure and a higher fraction of small pores with stronger boundaries is more resistant to external mechanical compressive stresses during cement loading. The needle-like particles in cements 1, 2 do not create dense microstructure, and it can be fractured under a lower load. Dissipation of energy during compressive loading is less effective around larger pores, especially in the case where the pore boundaries are composed of a low dense brittle cement matrix, which can breakthrough under loading. At such conditions, pores significantly support the fracture initiation and the local damage of the cement microstructure. In the case of DTS, there are strong effects of shear stresses along agglomerate or particle boundaries in cement microstructures. It is clear that the rough agglomerate boundaries with interconnected needle-like nanoparticles more intensively inhibited their mutual movement under tensile forces than smoother interphases or boundaries, where globular particles are not sufficiently bonded one to another. This fact can be the main reason of worse DTS values in cement 3.

CONCLUSION

TTCP powders after milling had the same irregular particle morphology as ones composed from pure tetracalcium phosphate phase. TTCP precursors differ by particle size distribution where a small fraction (up to 10 vol.%) of larger TTCP agglomerates were found in two samples, which were characterized by a bimodal distribution curve. The final cement phase after hardening in SBF was carbonated calcium-deficient nanohydroxyapatite with residua of TTCP and DCPA starting phases. Significant statistical differences were found in mechanical properties of three cement groups (various TTCP). From detailed analysis it resulted that a small content of larger TTCP agglomerates in starting cement mixtures had a strong effect on the cement microstructure formation and the morphology of nanohydroxyapatite particles. The different character of the microstructure is responsible for differences in mechanical properties of cements. The main problem in the preparation of TTCP precursors with comparable properties is milling partially sintered TTCP particles after annealing, because the particle size distribution is effectively influenced by milling process.

Acknowledgements

This work was realized within the framework of the project „Advanced implants seeded with stem cells for hard tissues regeneration and reconstruction“, which is supported by the Operational Program “Research and Development” financed through the European Regional Development Fund.

REFERENCES

[1] LeGeros, RZ., Chohayeb, A., Shulman, A.: J Dent Res, vol. 61, 1982, p. 343
[2] Brown, WE., Chow, LC.: J Dent Res, vol. 62, 1983, p. 672
[3] Chow, LC.: J Ceram Soc Jpn, vol. 99, 1991, p. 954
[4] Costantino, PD., Friedman, CD., Jones, K., Chow, LC., Pelzer, HJ., Sisson, GA.: Arch Otolaryngol Head Neck Surg, vol. 117, 1991, p. 379
[5] Liu, CS., Shen, W., Gu YF., et al.: J Biomed Mater Res, vol. 35, 1997, p.75
[6] Brown, WE., Chow, LC.: Dental restorative cement pastes. US Patent No. 4518430. May 21, 1985
[7] Ishikawa, K., Takagi, S., Chow, LC., Suzuki, K.: J Biomed Mater Res, vol. 46, 1999, p. 504

[8] Barralet, JE., Tremayne, MJ., Lilley, KJ., Gbureck, U.: Chem Mater, vol. 17, 2005, p. 1313
[9] Hirayama, S., Takagi, S., Markovic, M., Chow, LC.: J Res Natl Inst Stand Technol, vol. 113, 2008, p. 311
[10] Dagang, G., Kewei, X., Haoliang, S., Yong, H.: J Biomed Mater Res, vol. 77A, 2006, p. 313
[11] Burguera EF., Guitian, F., Chow, LC.: J Biomed Mater Res, vol. 71A, 2004, p. 275
[12] Medvecký, Ľ., Štulajterová, R., Briančin, J., Ďurišin, J.: Mater Sci Eng C, vol. 29, 2009, no. 8, p. 2493
[13] Tas, C.: Biomaterials, vol. 21, 2000, no. 14, p. 1429
[14] Dickens-Venz, SH., Takagi, S., Chow, LC., Bowen, RL., Johnston, AD., Dickens B.: Dent Mater, vol. 10, 1994, no. 2, p. 100
[15] Posset, U., Löcklin, E., Thull, R., Kiefer, W.: J Biomed Mater Res, vol. 40, 1998, p. 640
[16] Liao, CJ., Lin, FH., Chen, KS., Sun, JS.: Biomaterials, vol. 20, 1999, p. 1807
[17] Thamaraiselvi, TV., Prabakaran, K., Rajeswari, S.: Trends Biomater Artif Organs, vol. 19, 2006, no. 2, p. 81
[18] Matsuya, Y., Antonucci, JM., Matsuya, S., Takagi, S., Chow, LC.: Dent Mater, vol. 12, 1996, no. 1, p. 2